Development of high-resolution 72 h precipitation and hillslope flood maps over a tropical transboundary region by physically based numerical atmospheric–hydrologic modeling

T. Trinh, C. Ho, N. Do, A. Ercan and M. L. Kavvas

ABSTRACT

Long-term, high spatial and temporal resolution atmospheric and hydrologic data are crucial for water resource management. However, reliable high-quality precipitation and hydrologic data are not available in various regions around the world. This is, in particular, the case in transboundary regions, which have no formal data sharing agreement among countries. This study introduces an approach to construct long-term high-resolution extreme 72 h precipitation and hillslope flood maps over a tropical transboundary region by the coupled physical hydroclimate WEHY-WRF model. For the case study, Da and Thao River watersheds (D-TRW), within Vietnam and China, were selected. The WEHY-WRF model was set up over the target region based on ERA-20C reanalysis data and was calibrated based on existing ground observation data. After successfully configuring, WEHY-WRF is able to produce hourly atmospheric and hydrologic conditions at fine resolution over the target watersheds during 1900–2010. From the modeled 72 h precipitation and flood events, it can be seen that the main precipitation mechanism of DRW and TRW are both the summer monsoon and tropical cyclone. In addition, it can be concluded that heavy precipitation may not be the only reason to create an extreme flood event. The effects of topography, soil, and land use/cover also need to be considered in such nonlinear atmospheric and hydrologic processes. Last but not least, the long-term high-resolution extreme 72 h precipitation and hillslope flood maps over a tropical transboundary region, D-TRW, were constructed based on 111 largest annual historical events during 1900–2010.

Key words | Da-Thao river watershed, monsoon, transboundary region, tropical cyclone, watershed environmental hydrology (WEHY) model, weather research and forecasting model (WRF)

T. Trinh (corresponding author)
Faculty of Hydrology and Water Resources,
Thuy Loi University,
Hanoi,
Vietnam
E-mail: *tqtrinh@ucdavis.edu*

T. Trinh
M. L. Kavvas
Hydrologic Research Laboratory, Department of Civil and Environmental Engineering,
University of California,
Davis, CA,
USA

C. Ho
The Key Laboratory of River and Coastal Engineering, Hanoi,
Vietnam

N. Do
Vietnam Academy for Water Resources,
Hanoi,
Vietnam

A. Ercan
J. Amorocho Hydraulics Laboratory, Department of Civil and Environmental Engineering,
University of California,
Davis, CA,
USA

HIGHLIGHTS

- A physically based hydrology model coupled with a regional climate model is applied.
- Da-Thao river watersheds (D-TRW), within Vietnam and China, are selected.
- The extreme hydroclimate events were reconstructed during 1900–2010.
- Precipitation mechanisms of D-TRW are both the summer monsoon and tropical cyclone.
- The long-term high-resolution extreme 72 h precipitation and hillslope flood.

doi: 10.2166/wcc.2020.062

INTRODUCTION

Development of high-resolution long-term extreme precipitation and flood maps is a fundamental and challenging topic in the scientific research of water resources. Reliable precipitation and flood maps are necessary to ensure better water resource management and to support early identification of a range of natural disasters such as floods, flash-floods, landslides, and avalanches to serious cases of hail damage. According to Peruccacci *et al.* (2017), high-resolution precipitation maps were used in landslide susceptibility modeling to obtain landslide maps and spatial predictions of landslides in the whole of Italy. Bui *et al.* (2019) applied multivariate adaptive regression Splines and metaheuristic optimization with its input of flood, precipitation maps, and other influencing variables (elevation, slope, curvature, toposhade, aspect, topographic wetness index, stream power index, stream density, normalized difference vegetation index, soil type, and lithology) for predicting flash flood areas at tropical typhoon areas. Such landslide and flash flood maps rely on reliable high-quality precipitation and hydrologic data which are not available in various regions around the world (Kavvas *et al.* 2017). This is, in particular, the case in transboundary regions, which have no formal data sharing agreement among countries, leading to no or limited data availability. In spite of the importance of reliable high-resolution spatiotemporal precipitation and hydrologic maps, there is not yet a globally accepted standard approach.

Precipitation and flood maps can be obtained from ground measurements through weather stations (Yatagai *et al.* 2012; Daly *et al.* 2017). Ground stations are generally located at easily accessible and relatively low-elevation areas. In mountainous regions, the density of the observation network is usually low which prevents them from being used directly for local impact studies by conventional spatial interpolation techniques (Celleri *et al.* 2007; Ward *et al.* 2011; Kure *et al.* 2013; Arab Amiri *et al.* 2016). There have also been attempts to obtain precipitation maps from satellite remote sensing techniques (Melesse *et al.* 2007; Ceccherini *et al.* 2015). However, these satellites are not at high spatiotemporal resolution since the data are usually provided at the daily interval with spatial resolution generally larger than 25 km. Tan *et al.* (2015) evaluated six satellite and ground-based precipitation products over Malaysia from 2003 to 2007 and concluded that 3B42V7 (0.25°/daily) and APHRODITE (0.25°/daily) performed the best. Recently, Ho *et al.* (2018) dynamically downscaled ERA-20C reanalysis data to 9 km resolution over the Hong Thai Binh River watershed to investigate monthly precipitation and temperature during the 1950–2010 period and evaluated the trends by Mann–Kendall trend analysis.

A recent development that shows considerable promise is the regional climate model (RCM) coupled with a physically based hydrology model. This approach can generate more reliable spatial distribution maps of extreme precipitation and hillslope flood maps (Kure *et al.* 2013; Ishida *et al.* 2014; Trinh *et al.* 2016; Arab Amiri and Mesgari 2018; Toride *et al.* 2018). Kure *et al.* (2013) have used a distributed hydroclimate model, the Watershed Environmental Hydrology Hydro Climate Model (WEHY-HCM) (Chen *et al.* 2004a, 2004b; Kavvas *et al.* 2004, 2006; Kavvas *et al.* 2013), to reconstruct not only precipitation but also other variables such as temperature, wind speed, radiation, snowfall, snow melt, and streamflow at hourly intervals. WEHY-HCM uses large-scale atmospheric conditions for the lateral boundary conditions of its regional atmospheric module. Then, it simulates hydrological processes with the dynamically downscaled atmospheric data as the input. Although the distributed hydroclimate model can generate high-resolution precipitation and hillslope flood maps, the use of simulated hydroclimate data with limited duration can be misleading and may not represent the long-term conditions. One recommendation to decrease uncertainty is the use of long-term high-resolution datasets generated from a validated distributed hydroclimate model.

In this context, the study herein applies the distributed hydroclimate model with input provided from the European Centre for Medium-Range Weather Forecasts (ECMWF)–Atmospheric Reanalysis coarse climate data of the 20th century (ERA-20C) to develop long-term high-resolution 72 h precipitation and hillslope flood maps. The ERA-20C was selected since it provides three-dimensional data at 3-h time increments. This dataset is long enough, stable, and continuous and can uniformly cover the globe at a spatial resolution of 1.25° (approximately 165 km). The distributed hydroclimate model used in this study is the Weather Research and Forecasting (WRF, Skamarock *et al.* 2005) model coupled with a watershed hydrology, WEHY model. The previous version WEHY-HCM and current version WEHY-WRF hydroclimate model were considered and applied successfully in many regions around the world (Chen *et al.* 2016; Amin *et al.* 2017; Jang *et al.* 2017; Wuthiwongyothin *et al.* 2017; Gorguner *et al.* 2019; Ho *et al.* 2019). Thus, the proposed hydroclimate model is able to construct long-term extreme precipitation and flood maps over the target region.

The selected study regions, Da and Thao River watersheds (D-TRW), are two transboundary regions between China, Vietnam, and Laos. The upstream sector is located in China with 52.1% of the watershed area, while the downstream sector is located in Vietnam and Laos with 47.0 and 0.9% of the watershed area, respectively. The tropical mountainous regions of the watersheds are able to create extreme precipitation and flood by different atmospheric and orographic precipitation mechanisms (Frei & Schär 1998; Guan *et al.* 2005). In these regions, the water sources for heavy precipitation and flood are from summer monsoon (SMS) or tropical cyclone (TC) systems (Nguyen-Thi *et al.* 2012; Yokoi & Matsumoto 2008). Besides these mechanisms, orographic, soil moisture, and land use/cover effects also account for distributed surface, subsurface, and groundwater flows. In order to simulate accurately such a complex hydroclimate system, the WEHY-WRF needs to

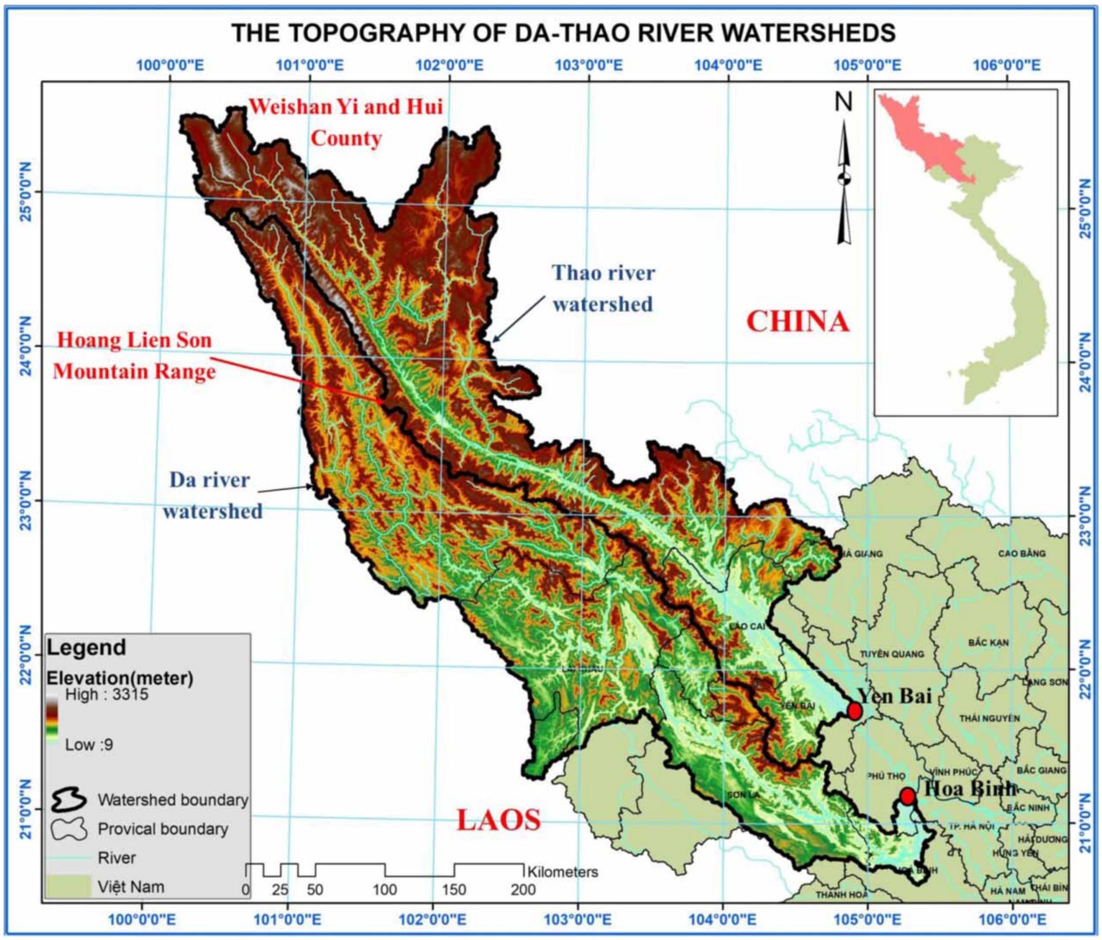

Figure 1 | Plan view of the Da-Thao River watersheds (The red points are outlet stations for the Da-Thao River watersheds). Please refer to the online version of this paper to see this figure in color: https://doi.org/10.2166/wcc.2020.062.

be validated before embarking on the construction of extreme precipitation and hillslope flood maps. After successfully configuring and evaluating, the WEHY-WRF model can construct tropical atmospheric and hydrologic mechanisms. Then, the long-term high-resolution extreme 72 h precipitation and hillslope flood maps over the tropical transboundary region, D-TRW, can be reconstructed at 9 km resolution during 1900–2010 by dynamically downscaling ERA-20C reanalysis data. Besides the investigation of 72 h precipitation and hillslope flood maps, orographic, soil moisture, and land use/cover effects are also assessed based on their impacts on flow conditions at the target watersheds. Consequently, the nonlinear interactions among atmospheric, land surface and flow processes are considered. Last but not least, this study provides a better understanding of the study region's hydrological regimes, especially the understanding of the timing and duration of hydro-meteorological hazards which are equally important for reducing socio-economic effects.

DESCRIPTION OF THE STUDY REGION

The Da and Thao Rivers are the two main stream tributaries of the Red River system, located in Northern Vietnam (downstream sector) and Southwest China (upstream

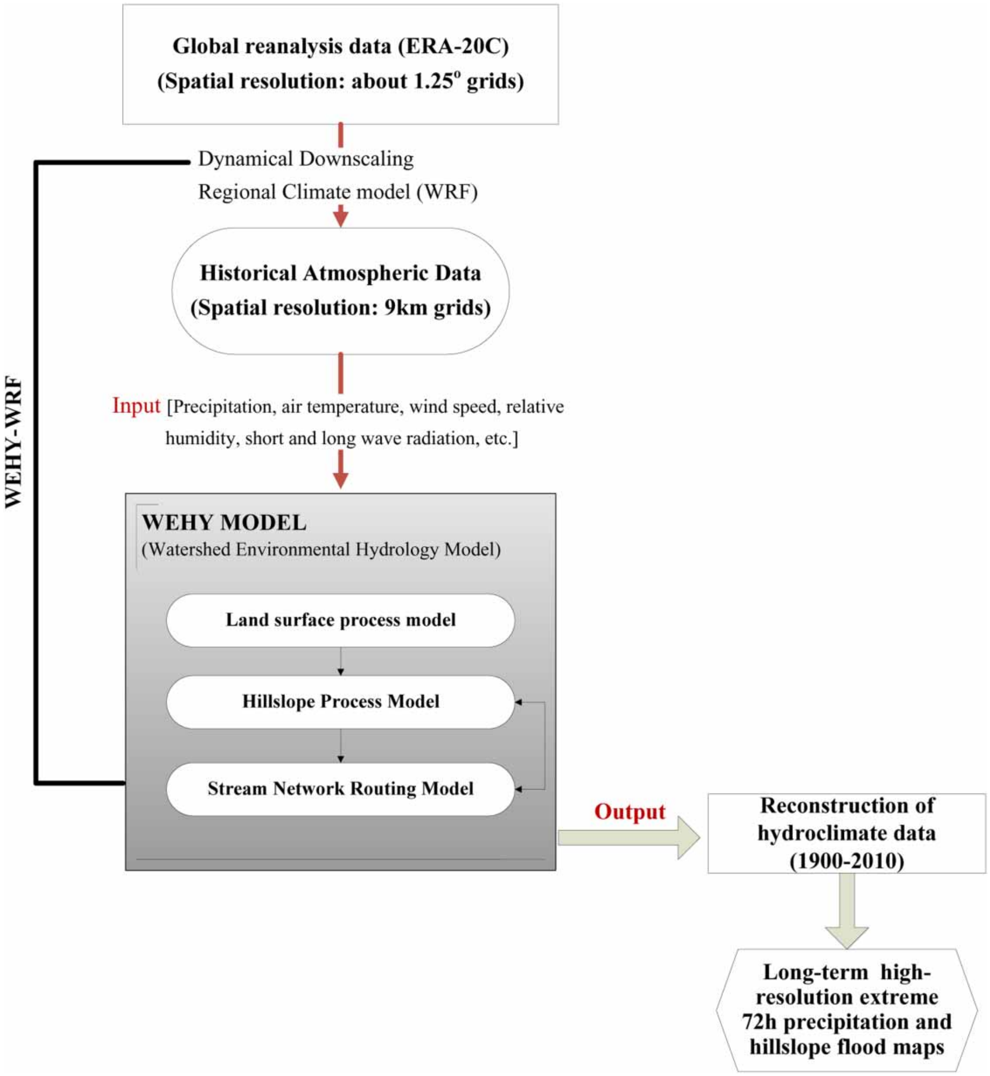

Figure 2 | Schematic description of the proposed methodology.

sector) with a catchment area of 99,550 km^2 (Figure 1). The upstream sector is located in China with 52.1% of the area, while the downstream sector is located in Vietnam with 47% of the area. The Thao River is the main stream of the Red River system, originating in Weishan Yi, and Hui Autonomous County, Yunnan Province, China, flows in a northwest-southeasterly direction through three Vietnamese provinces, including Lao Cai, Yen Bai, and Phu Tho. The main river branch is called Yuanjiang River in China and Thao in Vietnam. Thao River merges with Da River and Lo River at Viet Tri City, Phu Tho Province, Vietnam, before flowing into the Gulf of Tonkin in the East (East Sea). The second main stream is the Da River that is also known as Lixian River in China, and has a length of 440 km, while the downstream watershed is Da River with a length of 540 km. The Da River flows in an east-southerly

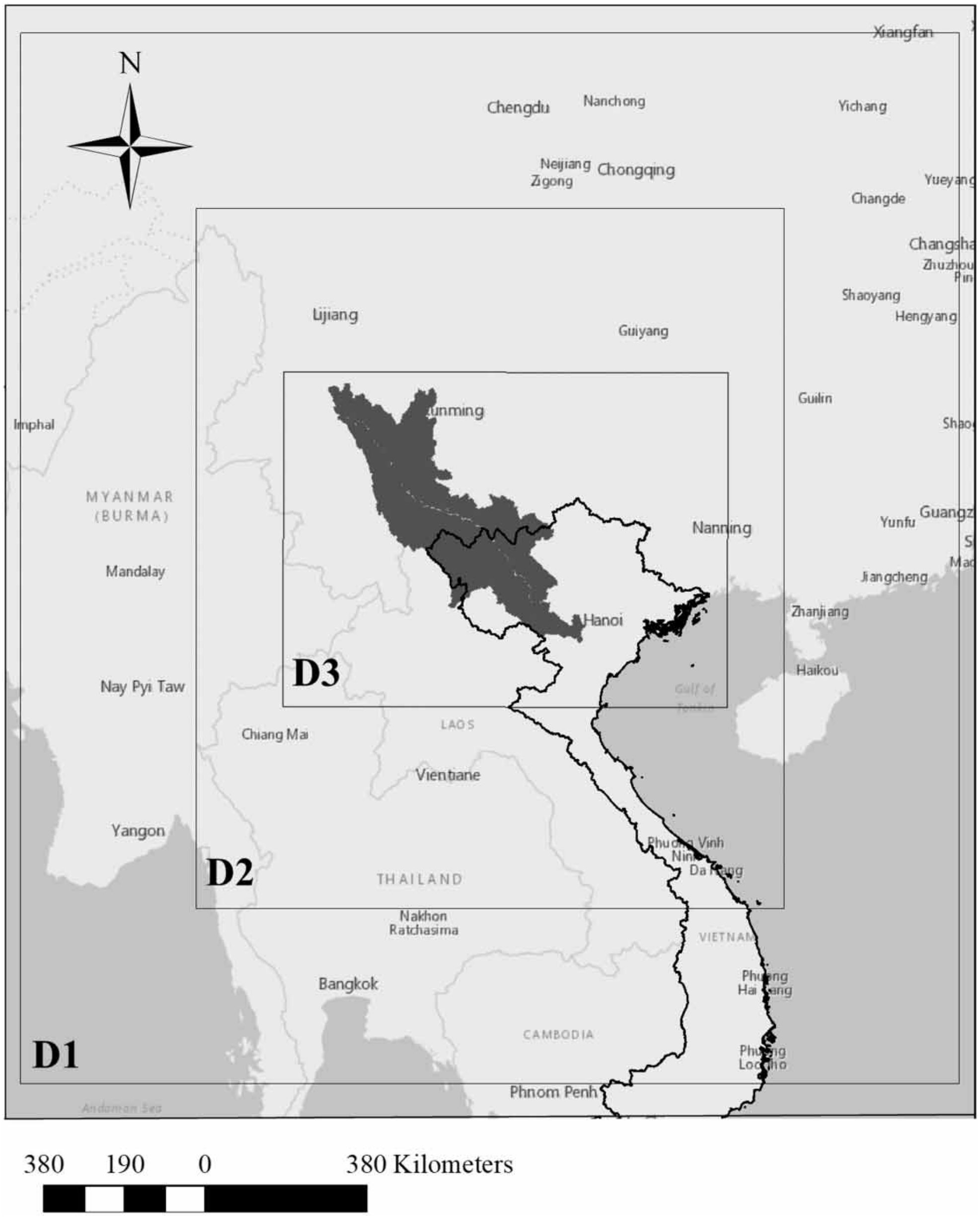

Figure 3 | Nested domains (D1 – 81 km; D2 – 27 km; and D3 – 9 km) for downscaling climate simulation over the D-TRW.

direction through Lai Chau, Dien Bien, Son La, Hoa Binh, and Phu Tho provinces, before merging with the Thao River at Tam Nong District near Viet Tri in Phu Tho Province. Within the D-TRW, Hoang Lien Son Mountains divide the D-TRW into Da and Thao River watersheds, which are the tributaries of the Red River. Due to its large area, average annual precipitation is spatially distributed in a wide range over D-TRW (from 100 to 1,800 mm during 1953–2013), and the rainy season lasting from May through October represents 85–90% of the total annual rainfall, and the dry season from November to April represents only 10–15% of the total annual rainfall (Le 2009). The flood season often occurs from June to mid-September over the D-TRW (flood peak magnitudes ranging from 2,000 to 12,000 cm); however, there are also some unusual flood peaks in October and November.

The land use and land cover over D-TRW are diverse. Mostly, the area is covered by forests, bare land, and crops. Forests and bare land cover 74% of the Da River watershed (DRW), and paddy rice fields cover 26% of the delta area. The Thao River watershed (TRW) is characterized by a larger diversity in land use including forest, paddy rice fields, and industrial crops (85%) (Ho et al. 2018).

METHODOLOGY

This study introduces a methodology to develop long-term high-resolution extreme 72 h precipitation and hillslope flood maps over a tropical transboundary region. This methodology can be implemented with any model although it is recommended to use a physically based hydroclimate model as mentioned in the 'Introduction' section. For the construction of high-resolution 72 h precipitation and hillslope flood maps over D-TRW, it is required to implement, calibrate, and validate the selected hydroclimate model over the D-TRW including upstream (in China) and downstream areas (in Vietnam). The schematic description of the historical hydrologic data reconstruction over D-TRW is shown in Figure 2. The input of the hydroclimate model is global atmospheric reanalysis dataset which is then dynamically downscaled by an RCM before being inputted into physical hydrologic model simulations. In this study, the European Centre for Medium-Range Weather Forecasts (ECMWF)–Atmospheric Reanalysis coarse climate data of the 20th century (ERA-20C) is selected due to its data quality and availability during the 1900–2010 period (Poli et al. 2013, 2015, 2016). The WRF model is used to downscale ERA-20C Reanalysis dataset for obtaining high-resolution atmospheric data during 1900–2010. The WRF is a physically based regional numerical atmospheric model that is able to provide high-resolution hydroclimate data that is well suited for the study of hydrologic extremes. As such, the methodology that uses WRF is appropriate to link with a watershed model because topography controls flow processes.

The dynamically downscaled atmospheric data covering both the upstream portion of the target watershed within China and the downstream portion within Vietnam were then processed and inputted into the hydrologic model, WEHY. The selected hydrologic model is a physically based hydrologic model that consists of two parts: the hillslope flow part and the channel routing part that are in dynamic interaction. The hillslope flow part of the module describes hydrologic processes through five components including unsaturated flow, subsurface stormflow, overland flow, groundwater flow, and channel flow on hillslopes (Chen et al. 2004a, 2004b; Kavvas et al. 2004, 2006, 2013).

Once successfully configured and validated, the WEHY-WRF can produce hourly atmospheric and hydrologic data, including precipitation, wind speed, water vapor flux, hillslope flow, and streamflow, among others. It is noted that the atmospheric fields can be obtained at all three configured domains (D1, D2, and D3), as shown in Figure 3; thus, it is possible to classify the large 72 h precipitation

Table 1 | WRF model configuration (Ho et al. 2018)

WRF model configuration	Selected option
Microphysics processes	Goddard scheme (Tao et al. 1989)
Cumulus parameterization	New Simplified Arakawa–Schubert scheme (Han & Pan 2011)
Planetary boundary layer scheme	BouLac scheme (Bougeault & Lacarrere 1989)
Radiation scheme	New Goddard scheme (Chou & Suarez 1999)
Surface scheme	RUC land surface model (Benjamin et al. 2004)

mechanisms (SMS or TCs) for each target watershed. Along with atmospheric spatial maps, the physical watershed model-WEHY also produces the flow over hillslopes. Therefore, both spatial precipitation and flow maps can be generated. In addition, since the constructed hydroclimate data are available for 111 years (1900–2010), it is possible to analyze such historical fine spatiotemporal atmospheric–hydrologic data by means of statistical and spatial analyses. Such information is meant for strategic planning in water resources management.

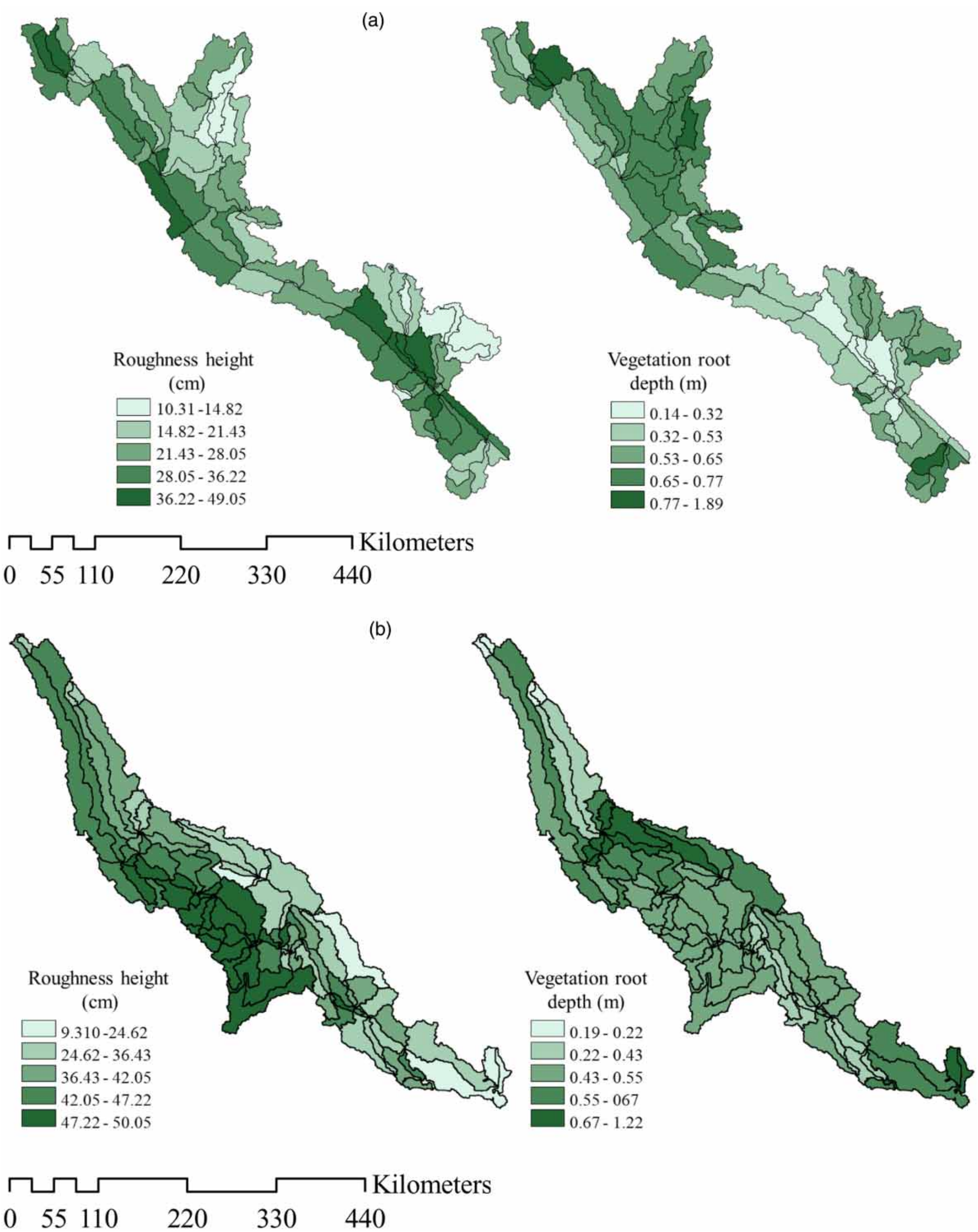

Figure 4 | Estimated land surface parameter maps for (a) Thao and (b) Da River watersheds.

DATA AND MODEL IMPLEMENTATION

The historical reanalysis data, ERA-20C, were utilized to set up the initial and boundary conditions of the RCM, Weather Research and Forecasting Model (WRF, Skamarock et al. 2005), to dynamically downscale atmospheric variables over Da and Thao watersheds as reported in Ho et al. (2018). Through a series of nested domains, WRF successfully downscaled the ERA-20C from 1.25° (approximately 165 km) grid resolution, to cells at 9 km by 9 km grid resolution at hourly

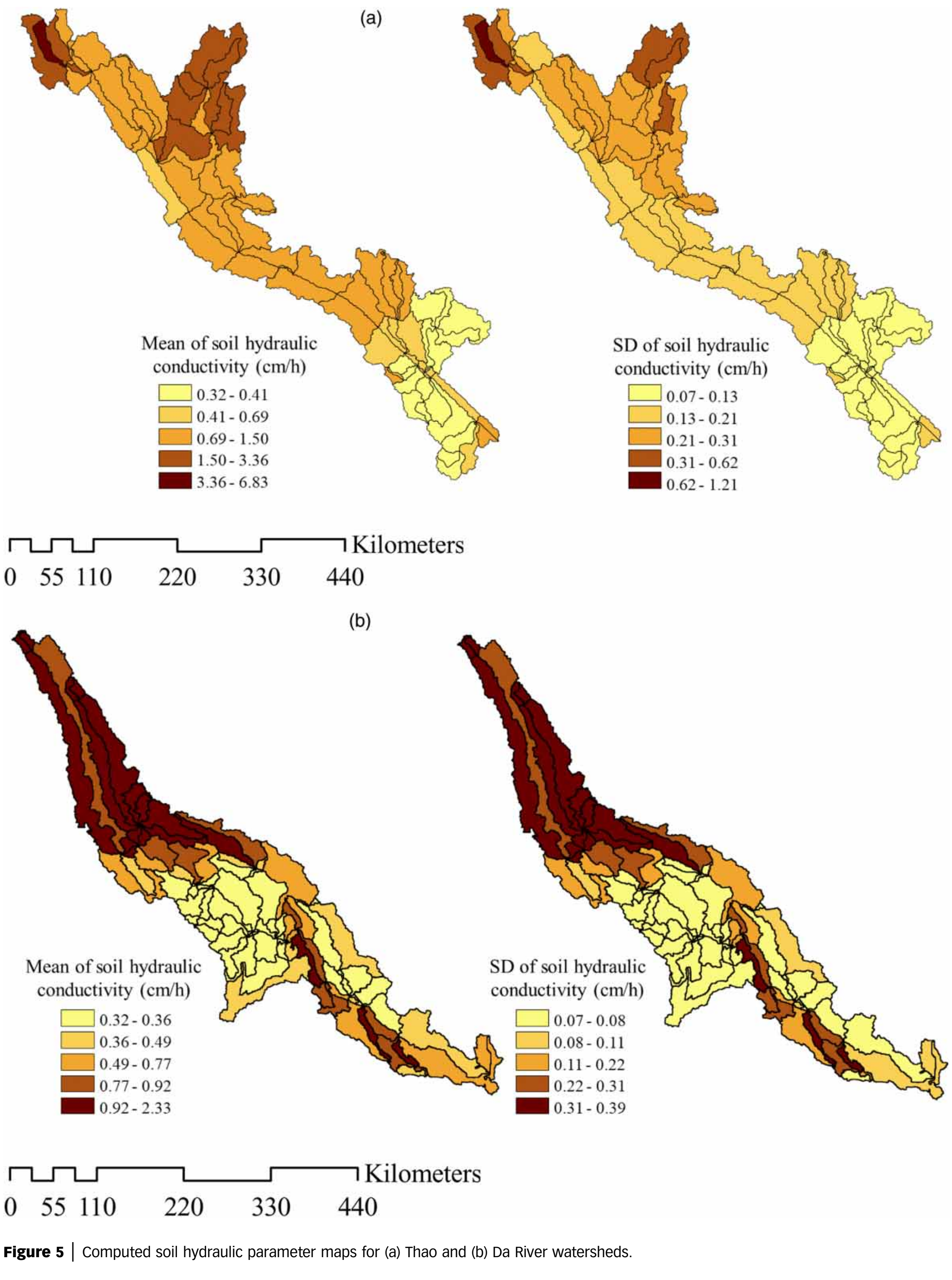

Figure 5 | Computed soil hydraulic parameter maps for (a) Thao and (b) Da River watersheds.

intervals. The spatial resolution of each domain is one-third of its parent domain; the first domain (D1) has a spatial grid resolution of 81 km, the second (D2) is 27 km, and the third (D3) is 9 km (Figure 3). Table 1 shows the WRF configuration of the physics options used in this study.

By downscaling coarse resolution ERA-20C reanalysis climate data, the atmospheric inputs including precipitation, temperature, wind speed, shortwave radiation, longwave radiation, pressure, mixing ratio, and geopotential height were processed to be used as input to WEHY model applications.

Along with atmospheric data, the topography, soil, and land use/cover information were also implemented in the hydrologic model. Such information cannot be assumed without any upstream data information. The topography parameters were delineated from the ASTER Global DEM with spatial resolution of 30 m (Tachikawa *et al.* 2011). Soil parameters were delineated from the SoilGrids of 1 km resolution (Hengl *et al.* 2014; Trinh *et al.* 2018), and land use/cover was retrieved from Global Land Cover Characterization of 1 km resolution (GLCC) dataset (Loveland *et al.* 2000). These parameters were estimated through the processing of Geographical Information System (GIS) data before integrating with atmospheric data into model computational units (MCUs) (Kavvas *et al.* 2013).

By applying the GIS technique on the ASTER Global DEM, the delineation products including 78 MCUs and 39 stream reaches were extracted for TRW and 92 MCUs and 46 stream reaches for DRW. Estimations of geomorphologic, soil properties, and land surface parameters for MCUs of the WEHY are shown in Figures 4 and 5. As explained in Chen *et al.* (2004a), stationary heterogeneity of parameters within a hillslope was assumed. Consequently, the same mean and variance values of the parameters at the hillslope scale were used for all transects within that hillslope.

For hydrologic process validation, the simulated runoff from the hydrologic model was compared with the corresponding observations. This study used a 7-year period, from 1975 to 1981, for the model calibration, and a 3-year period, from 1982 to 1984, for model validation. Calibration and validation of the daily mean discharges at Yen Bai station, the outlet of TRW, and Hoa Binh station, the outlet of DRW, are presented in Figure 6. The visual comparison between the model simulations and corresponding observations shows that they

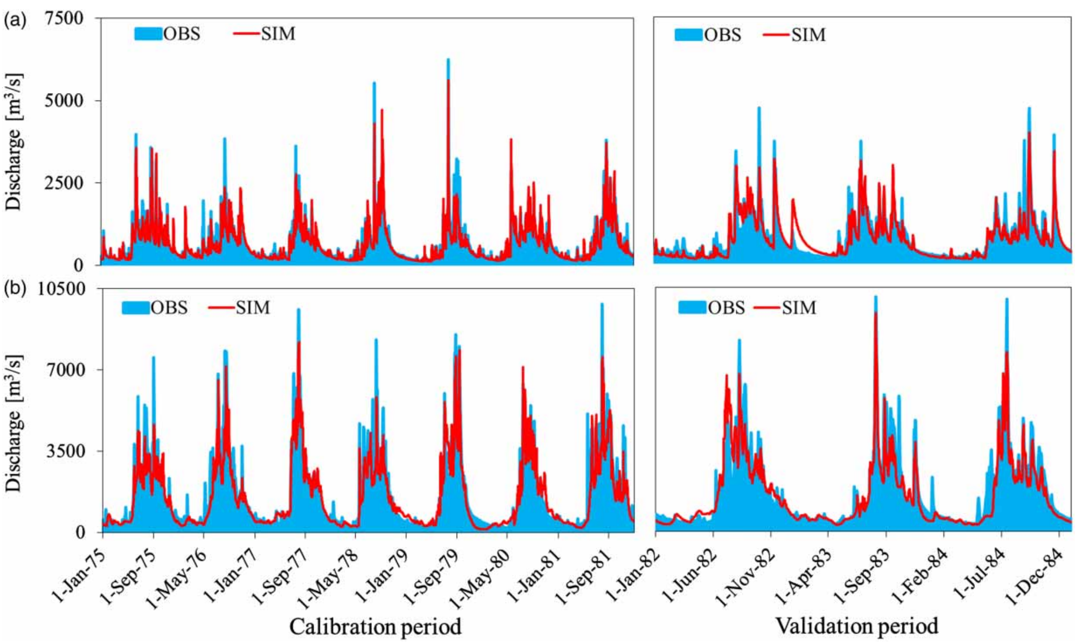

Figure 6 | Comparison of the daily mean discharge by WEHY simulations and the corresponding observations at (a) Yen Bai in TRW and (b) Hoa Binh in DRW.

match quite well for both watersheds. The rising and recession segments of the simulated hydrographs, as well as the timing of the simulated peak discharges, are very similar to the corresponding observations. Although the simulated peak discharges sometimes underestimate the observed data, the differences are not so large. Table 2 lists the performance statistics for the WEHY hydrology model application over the D-TRW. The simulated data are in good agreement with the observed data because the mean and standard deviation values are similar, and the correlation coefficient, as well as the Nash-Sutcliffe efficiency, is sufficiently high (close to 1).

Table 2 | Daily streamflow calibration and validation results at the watershed outlet locations, Yen Bai station in TRW and Hoa Binh station in DRW

	Yen Bai station		Hoa Binh station	
Flow statistics	**Calibration (1975–1981)**	**Validation (1982–1984)**	**Calibration (1975–1981)**	**Validation (1982–1984)**
Mean by observation (m^3/s)	648.04	729.06	1566.08	1637.48
Mean by simulation (m^3/s)	637.41	727.01	1540.61	1541.13
Standard deviation by observation	567.14	623.89	1453.07	1561.28
Standard deviation by simulation	574.79	617.94	1440.14	1369.19
Nash coefficient	0.757	0.767	0.821	0.824
Correlation coefficient	0.882	0.870	0.911	0.902

Discussion and development of historical 72 h precipitation and flood over D-TRW.

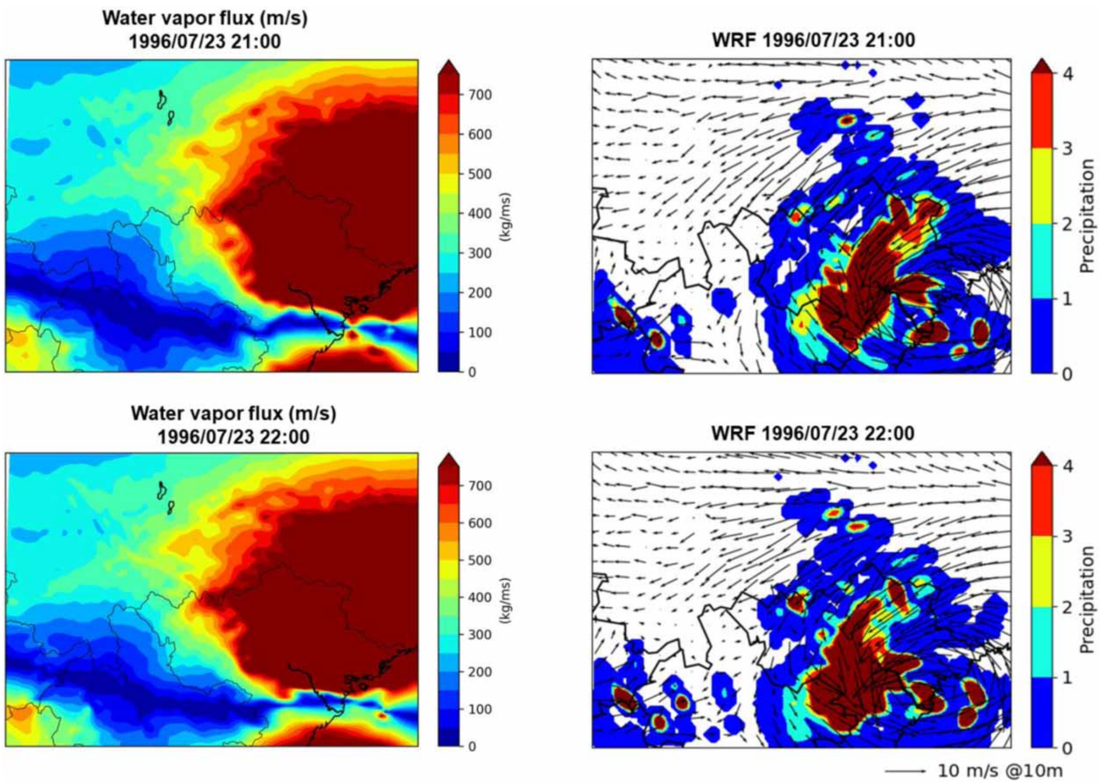

Figure 7 | Water vapor flux (kg/m s) on the left and precipitation (mm) with wind speed vector (m/s) at 10 m (above the ground) on the right for the 1996 event over the DRW (domain 3).

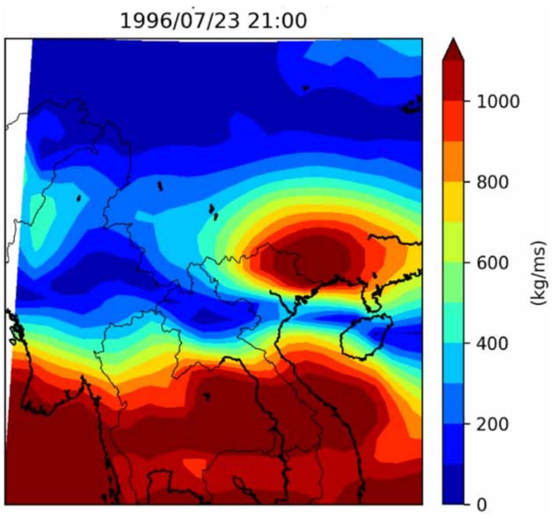

Figure 8 | Water vapor flux (kg/m s) map for the 1996 event over the DRW (domain 1).

RESULTS AND DISCUSSION

After configuring the selected hydroclimate WEHY-WRF model, the historical precipitation and hydrologic data were reconstructed from 1900 to 2010. The maximum 72 h basin-average precipitation in a water year were extracted and ranked over the Da and Thao River watersheds.

Although both Da and Thao River watersheds were located in the Red River system, their large 72 h historical events were different in time and contributed percentage from Vietnam territory. It is noted that the average precipitation contribution from the Vietnam territory for TRW was 61.6%, while that for DRW was 50.25%.

In order to evaluate the precipitation mechanisms for both watersheds, the water vapor flux and precipitation with wind speed were investigated for WRF domains. Figure 7 shows the water vapor flux and precipitation with wind speed vectors at 10 m above the ground for the largest 72 h historical storm event over the DRW (domain 3). It is noted that the water vapor flux came from southeast of the simulated domains and moved to the southeast-northwesterly direction through DRW. The main water vapor flux direction was southwest-northwesterly that is shown clearly over domain 1 in Figure 8. The precipitation mechanism of

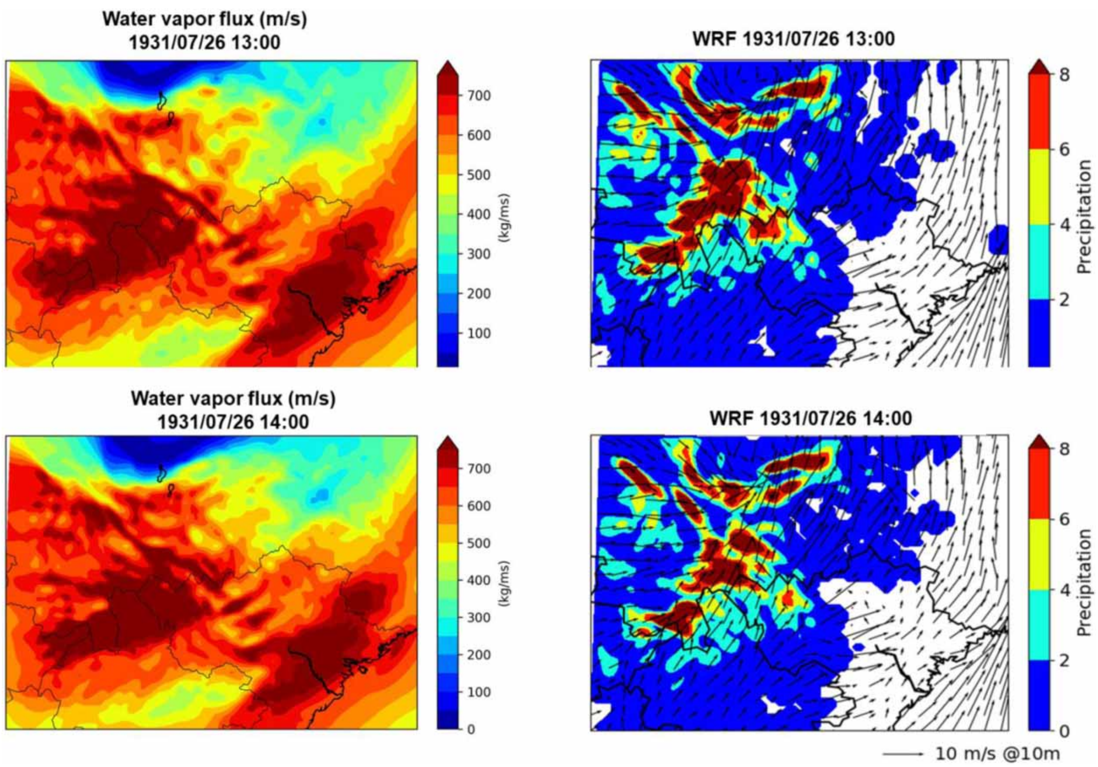

Figure 9 | Water vapor flux (kg/m s) on the left and precipitation (mm) with wind speed vector (m/s) at 10 m (above the ground) on the right for the 1931 event over the DRW (domain 3).

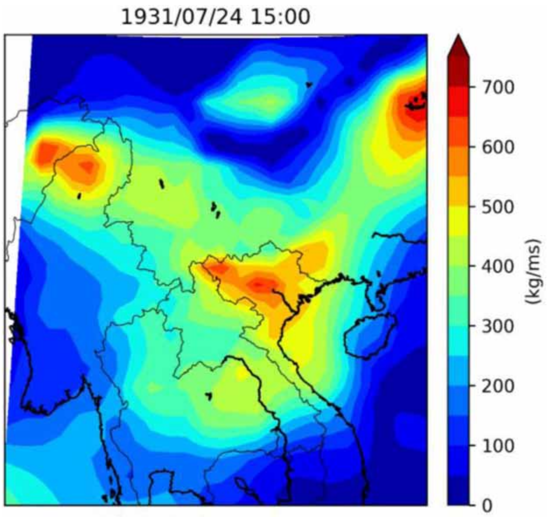

Figure 10 | Water vapor flux (kg/m s) map for the 1931 event over the DRW (domain 1).

the event was created by TC from the East Sea of Vietnam and moves toward the D-TRW.

Figure 9 shows the water vapor flux and precipitation with wind speed vectors at 10 m for the second largest 72 h storm event over the DRW (domain 3). The water vapor flux came from monsoon system in the southwest, northwest, and northeast of the simulated domains and moved to the target watershed, creating heavy rainfall in July (Figure 10). The precipitation mechanism of the event was created by three different moisture sources.

Figure 11 shows MCU averaged 72 h precipitation obtained from the average of 111 largest annual historical events during 1900–2010 over the DRW. The heavy 72 h precipitation is located around the Vietnam and China border region with the precipitation amount up to 331 mm.

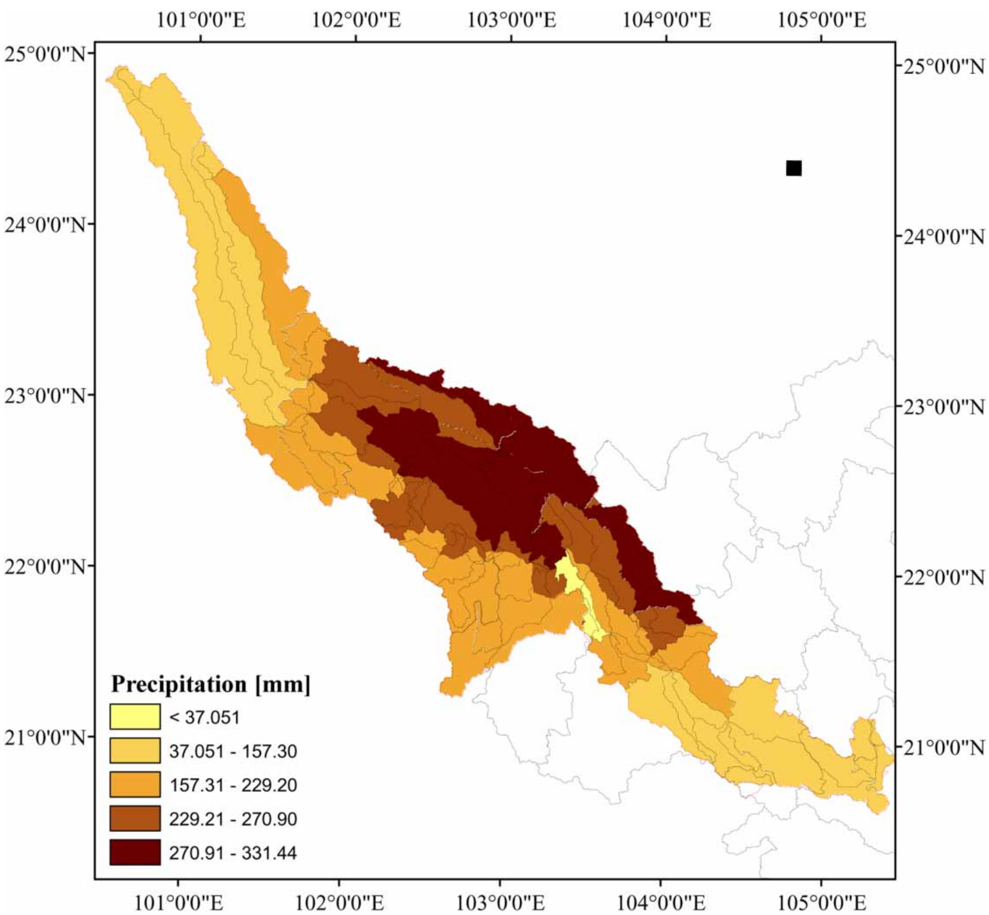

Figure 11 | The MCU averaged 72 h precipitation map obtained from the averaged 111 largest annual historical events during 1900–2010 over the DRW.

For the TRW, the water vapor flux and precipitation with wind speed vectors at 10 m for the largest and second largest 72 h historical storm event (domain 3) are shown in Figures 12 and 13, respectively. The heavy rainfall can be created by SMS and TC. In the case of the 1989 event, the large moisture came from south of the simulated domains and moved to DRW before reaching the Hoang Lien Son mountain range. Theoretically, such moisture can create a heavy precipitation volume over the Da River area. However, this moisture went through the Hoang Lien Son mountain range at low-elevation regions before merging with the moisture from the north and creating a large rainfall event over the TRW.

In the 1971 event, the heavy precipitation was created by a TC (Figure 13). This TC was originated from the East Sea of Vietnam and moved to TRW before hitting the Hoang Lien Son mountain range, creating a heavy rainfall event in here. Due to the TC's starting location and moving direction, the heavy precipitation of 1971 event fell more in the downstream (in Vietnam) than the upstream sector (in China) with 65% rain falling in Vietnam territory. Such information also confirms the differences between atmospheric conditions at Da and Thao River watersheds. Figure 14 shows MCU averaged 72 h precipitation obtained from the 111 largest annual historical events during 1900–2010 over the TRW. This figure shows that the heavy 72 h precipitation is located over the Vietnam territory with a precipitation amount of up to 331 mm.

After successfully reconstructing the climate data over the D-TRW by the WRF model, the WEHY model was then utilized to obtain hydrologic conditions from 1900 to 2010 using the calibrated model parameters. The historical extreme flow events were extracted for each year with respect to 72 h flow volume equivalent depth over the Da and Thao River watersheds. Event periods were determined by the largest 72 h flow volume.

In order to investigate the effects of land surface variables, Figures 15 and 16 depict the MCU averaged 72 h heaviest precipitation and hillslope flow maps obtained

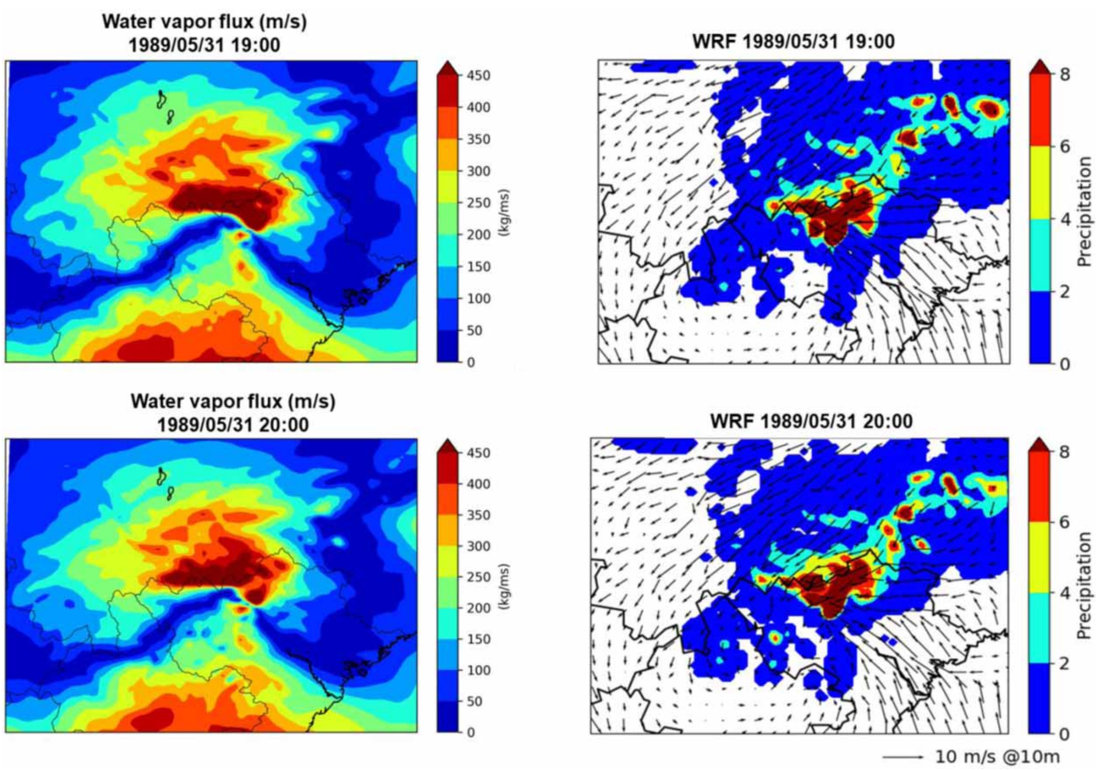

Figure 12 | Water vapor flux (kg/m s) on the left and precipitation (mm) with wind speed vector (m/s) at 10 m (above the ground) on the right for the 1989 event over the Thao River watershed (domain 3).

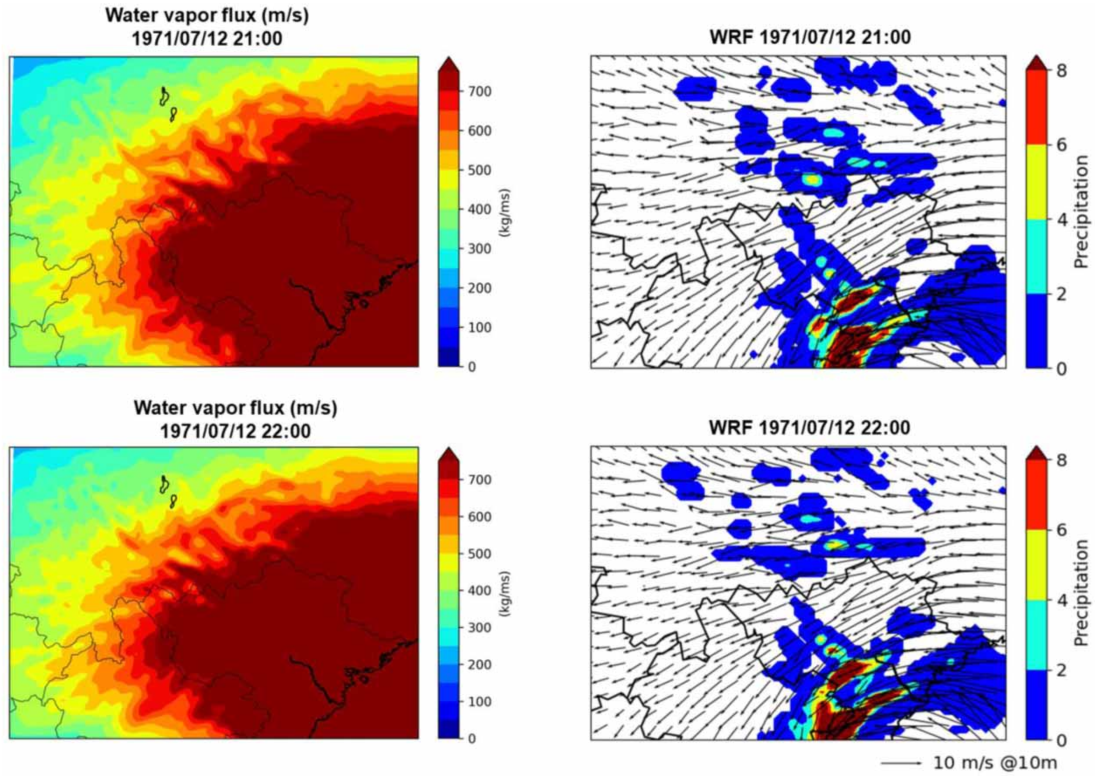

Figure 13 | Water vapor flux (kg/m s) on the left and precipitation (mm) with wind speed vector (m/s) at 10 m on the right for the 1971 event over Thao River watershed (domain 3).

from the 111 largest annual historical events during 1900–2010 over the Da and Thao River watersheds. As can be seen from both figures, the spatial distributions of precipitation and hillslope flow are different. The hillslope flow over DRW is largest at hillslopes at the upstream sector, where the precipitation depth was not so large. The hillslope flow of TRW was larger at hillslopes closer to the Hoang Lien Son mountain range in the northwest of the watershed, while the heavy precipitation mostly occurs downstream in the southeast of the watershed in Vietnam.

Overall, the long-term high-resolution historical maximum 72 h precipitation depths over a tropical transboundary region, Da-Thao River watersheds, were spatial resolution of each of the nested domains is one-third of that of its parent domain; the first domain (D1) has a spatial grid resolution of 81 km, the second (D2) is 27 km, and the third (D3) is 9 km constructed and mapped as shown in Figure 17. The long-term hillslope flood maps for D-TRW were also constructed as shown in Figure 18. Such information is useful for strategic planning and climate change adaptation in the water resources management and flood protection of the D-TRW.

CONCLUSIONS

In this study, historical interactive atmospheric–hydrologic events were reconstructed over the D-TRW, the two transboundary watersheds with very limited data or no data from their upstream sector, using a RCM coupled with a hydrology model (WEHY-WRF). The historical atmospheric data were constructed by the WRF model with its inputs provided from the reanalysis ERA-20C with spatial resolution of 1.25 (~165 km) at 3-h time increments. After its successful reconfiguration, WEHY-WRF was able to reconstruct historical hourly atmospheric hydrologic conditions at fine spatial resolution over the target watersheds during 1900–2010. The numerical atmospheric–hydrologic modeling method, presented in this study for the possible estimation

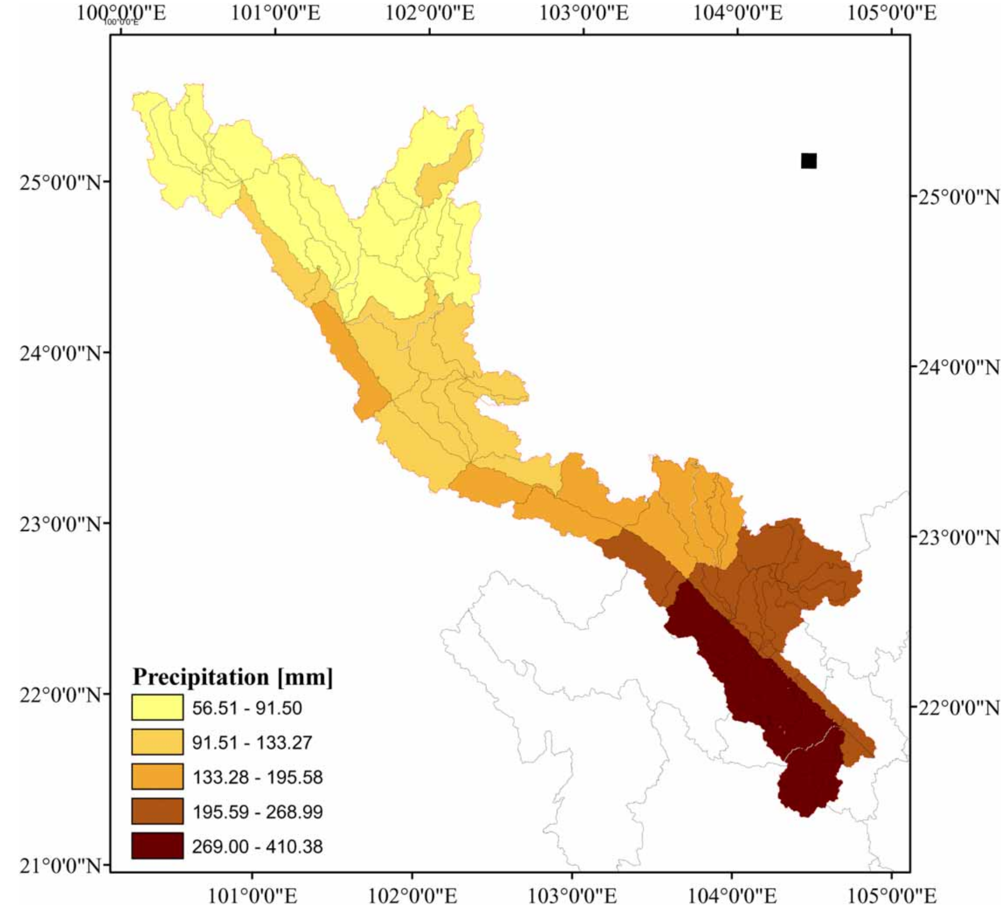

Figure 14 | The MCU averaged 72 h precipitation map obtained from the averaged 111 largest annual historical events during 1900–2010 over the Thao River watershed.

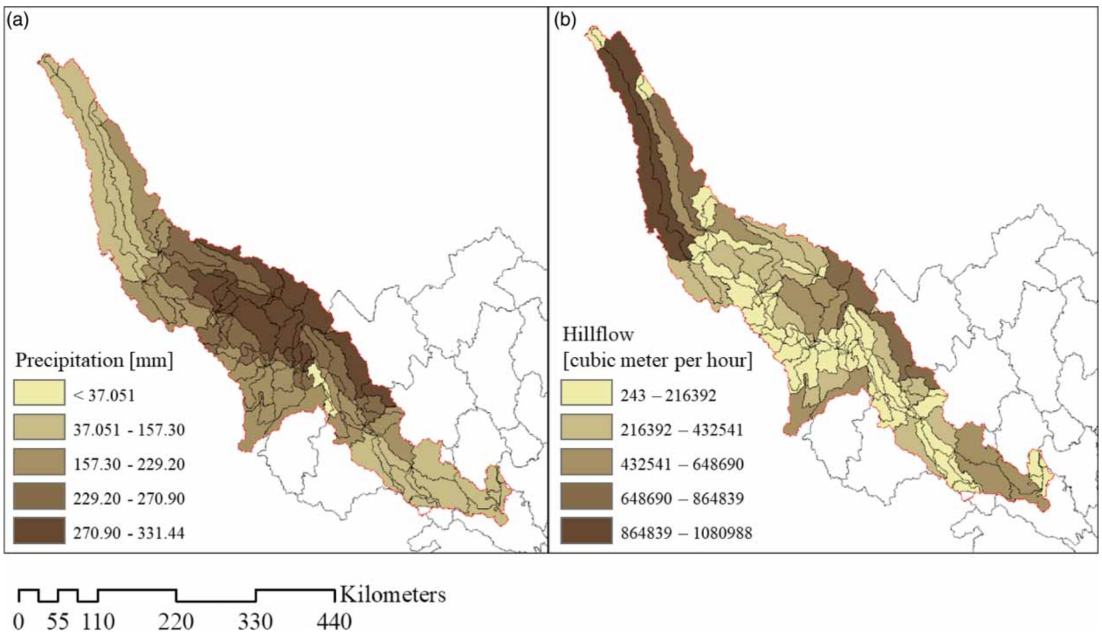

Figure 15 | The MCU averaged 72 h heavy precipitation map (a) and hillslope flow map (b) obtained from the 111 largest annual historical events during 1900–2010 over the DRW.

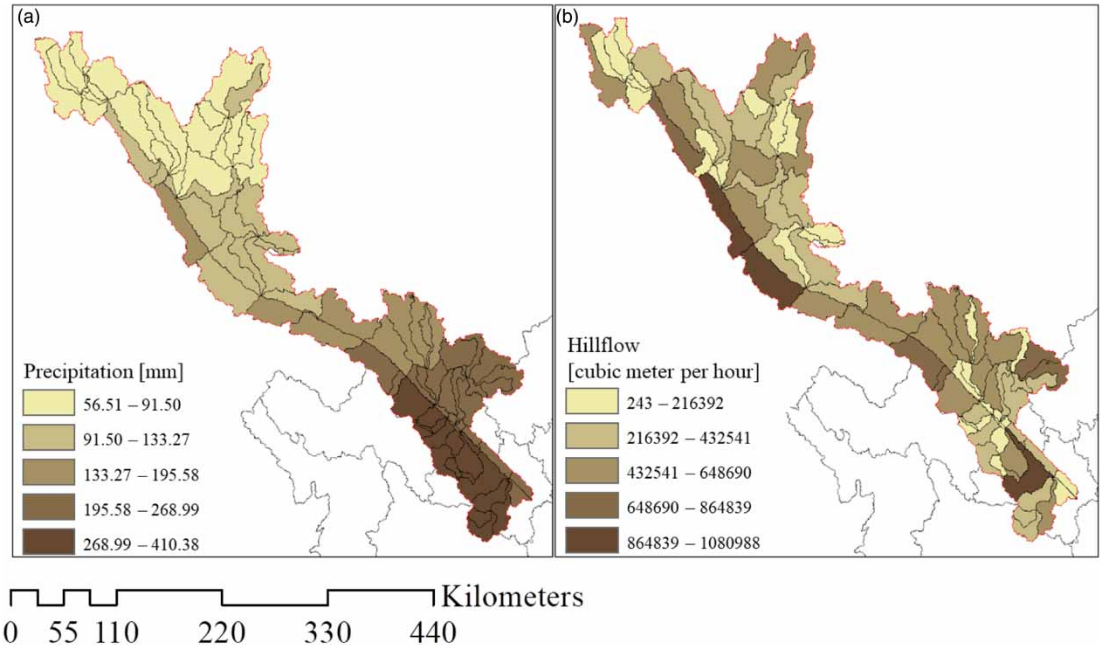

Figure 16 | The MCU averaged 72 h heaviest precipitation map (a) and hillslope flow map (b) obtained from the 111 largest annual historical events during 1900–2010 over the Thao River watershed.

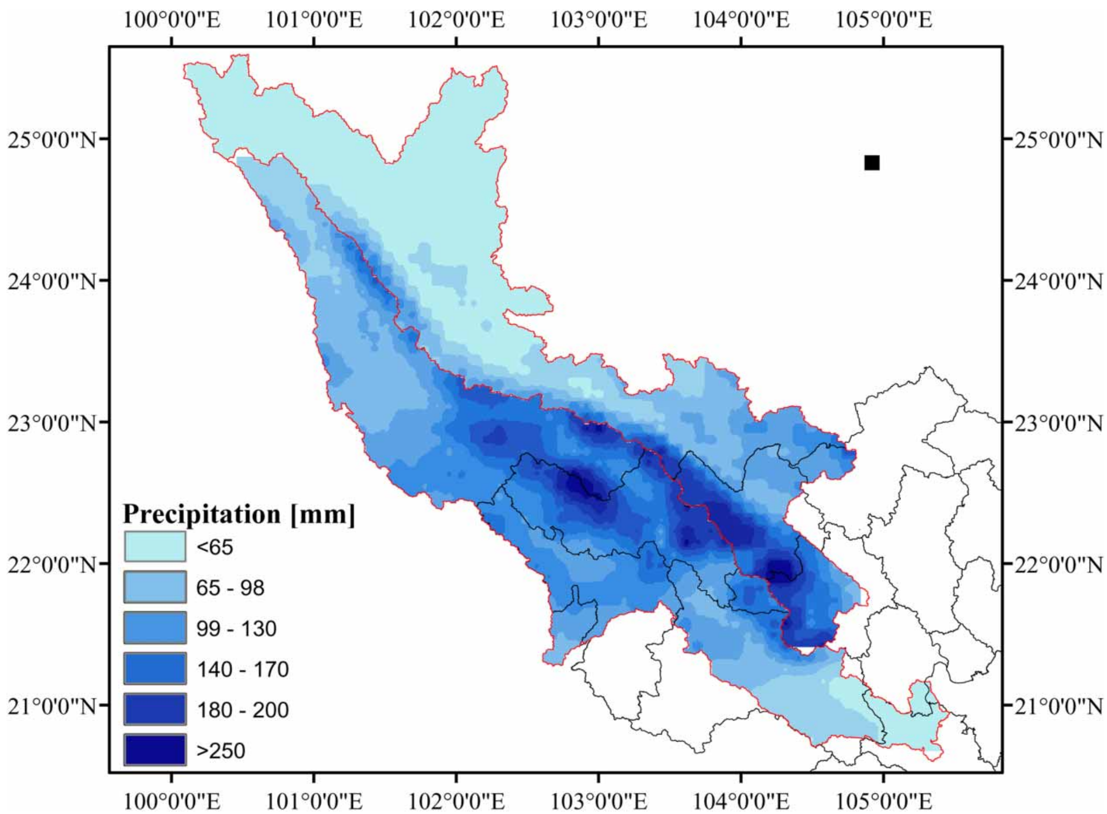

Figure 17 | The long-term high-resolution extreme 72 h precipitation depths obtained from the 111 largest annual historical events during 1900–2010 over D-TRW.

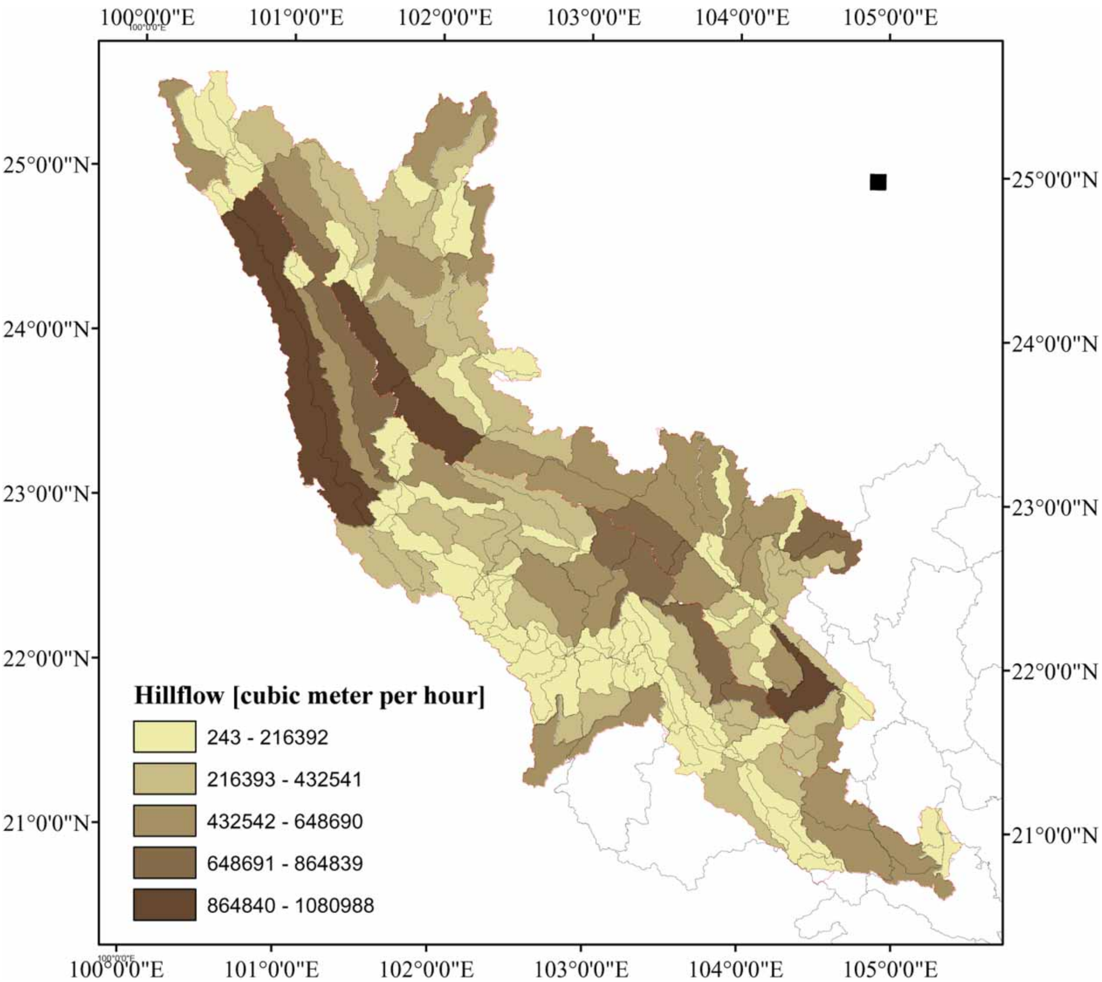

Figure 18 | The MCU (hillslope) averaged 72 h hillslope flow map obtained from the 111 largest annual historical events during 1900–2010 over D-TRW.

of heavy precipitation and flood events over the two target watersheds, does provide a comprehensive physical approach that can explain the effects of atmospheric–hydrologic and topographic conditions, in time and space over a target watershed.

The historical precipitation and flood events were extracted for each water year with respect to the largest 72 h basin-average precipitation and 72 h flow volume equivalent depth over the Da and Thao River watersheds during 1900–2010. From the modeled 72 h precipitation and flood events, it can be seen that the main precipitation mechanisms of DRW and TRW are by either SMS or TC that brings a humid climate and torrential rainfall to this area, as can be seen in Figures 8, 10, 12, and 13. In addition, it can be concluded that a large precipitation event may not be the only factor in creating a large flood event. As can be seen from Figures 15 and 16, the largest precipitation event does not necessarily correspond to the largest flow. Thus, it is necessary to account for the effects of topography, soil, and land use/cover in the nonlinear interaction of atmospheric and hydrologic processes. Based on the reconstructed hourly precipitation and hillslope flow data, it is possible to construct long-term high-resolution extreme 72 h precipitation depth and hillslope flood maps over Da-Thao River watersheds, as shown in Figures 17 and 18. As can be seen from both figures, the spatial distributions of precipitation depths and hillslope flows are different. This result again confirms the previous conclusion that the largest precipitation event does not necessarily result in the largest flood event.

The results of this study can then be used for both short- and long-term water resources and flood management since it could provide hourly hydroclimate data that can be converted into daily and monthly data. Along with long-term high-resolution extreme 72 h precipitation and hillslope flood maps, this approach allows us to simulate the relevant atmospheric and hydrologic variables under different land surface conditions. Hence, it is possible to assess orographic, soil moisture, and land use/cover effects on the flow conditions at the target watersheds. Last but not least, this study introduces a modeling approach that can generate reliable high-quality precipitation and hydrologic data which are not available in various regions around the world.

ACKNOWLEDGEMENTS

This study was financially supported by the Fostering Innovation through Research, Science and Technology Project (FIRST), Vietnamese Ministry of Science and Technology and World Bank. The study was implemented at the Key Laboratory of River and Coastal Engineering (KOLRCE-Vietnam).

DATA AVAILABILITY STATEMENT

All relevant data are included in the paper or its Supplementary Information.

REFERENCES

Amin, M. Z. M., Shaaban, A. J., Ercan, A., Ishida, K., Kavvas, M. L., Chen, Z. Q. & Jang, S. 2017 Future climate change impact assessment of watershed scale hydrologic processes in Peninsular Malaysia by a regional climate model coupled with a physically-based hydrology models. *Science of the Total Environment* **575**, 12–22.

Arab Amiri, M. & Mesgari, M. S. 2018 Analyzing the spatial variability of precipitation extremes along longitude and latitude, northwest Iran. *Kuwait Journal of Science* **45** (1), 121–127.

Arab Amiri, M., Amerian, Y. & Mesgari, M. S. 2016 Spatial and temporal monthly precipitation forecasting using wavelet transform and neural networks, Qara-Qum catchment, Iran. *Arabian Journal of Geosciences* **9** (5), 1–18. doi:10.1007/s12517-016-2446-2.

Benjamin, S. G., Dévényi, D., Weygandt, S. S., Brundage, K. J., Brown, J. M., Grell, G. A., Kim, D., Schwartz, B. E., Smirnova, T. G., Smith, T. L. & Manikin, G. S. 2004 An hourly assimilation–forecast cycle: the RUC. *Monthly Weather Review* **132** (2), 495–518.

Bougeault, P. & Lacarrere, P. 1989 Parameterization of orography-induced turbulence in a mesobeta-scale model. *Monthly Weather Review* **117** (8), 1872–1890.

Bui, D. T., Hoang, N. D., Pham, T. D., Ngo, P. T. T., Hoa, P. V., Minh, N. Q., Tran, X. T. & Samui, P. 2019 A new intelligence approach based on GIS-based multivariate adaptive regression splines and metaheuristic optimization for predicting flash flood susceptible areas at high-frequency tropical typhoon area. *Journal of Hydrology* **575**, 314–326.

Ceccherini, G., Ameztoy, I., Hernández, C. & Moreno, C. 2015 High-resolution precipitation datasets in South America and West Africa based on satellite-derived rainfall, enhanced vegetation index and digital elevation model. *Remote Sensing* **7** (5), 6454–6488.

Celleri, R., Willems, P., Buytaert, W. & Feyen, J. 2007 Space–time rainfall variability in the Paute basin, Ecuadorian Andes. *Hydrological Processes* **21** (24), 3316–3327.

Chen, Z. Q., Kavvas, M. L., Fukami, K., Yoshitani, J. & Matsuura, T. 2004a Watershed environmental hydrology (WEHY) model: model application. *Journal of Hydrologic Engineering* **9** (6), 480–490.

Chen, Z. Q., Kavvas, M. L., Yoon, J. Y., Dogrul, E. C., Fukami, K., Yoshitani, J. & Matsuura, T. 2004b Geomorphologic and soil hydraulic parameters for watershed environmental hydrology (WEHY) model. *Journal of Hydrologic Engineering* **9** (6), 465–479.

Chen, J., Kavvas, M. L., Ishida, K., Trinh, T., Ohara, N., Anderson, M. L. & Chen, Z. R. 2016 Role of snowmelt in determining whether the maximum precipitation always results in the maximum flood. *Journal of Hydrologic Engineering* **21** (10), 04016032.

Chou, M. D. & Suarez, M. J. 1999 *A Solar Radiation Parameterization (CLIRAD-SW) for Atmospheric Studies*. NASA Technical Memorandum 10460, 48.

Daly, C., Slater, M. E., Roberti, J. A., Laseter, S. H. & Swift Jr, L. W. 2017 High-resolution precipitation mapping in a mountainous watershed: ground truth for evaluating uncertainty in a national precipitation dataset. *International Journal of Climatology* **37**, 124–137.

Frei, C. & Schär, C. 1998 A precipitation climatology of the Alps from high-resolution rain-gauge observations. *International Journal of Climatology* **18** (8), 873–900.

Gorguner, M., Kavvas, M. L. & Ishida, K. 2019 Assessing the impacts of future climate change on the hydroclimatology of the Gediz Basin in Turkey by using dynamically downscaled CMIP5 projections. *Science of the Total Environment* **648**, 481–499.

Guan, H., Wilson, J. L. & Makhnin, O. 2005 Geostatistical mapping of mountain precipitation incorporating autosearched effects of terrain and climatic characteristics. *Journal of Hydrometeorology* **6** (6), 1018–1031.

Han, J. & Pan, H. L. 2011 Revision of convection and vertical diffusion schemes in the NCEP global forecast system. *Weather and Forecasting* **26** (4), 520–533.

Hengl, T., de Jesus, J. M., MacMillan, R. A., Batjes, N. H., Heuvelink, G. B., Ribeiro, E., Samuel-Rosa, A., Kempen, B., Leenaars, J. G., Walsh, M. G. & Gonzalez, M. R. 2014 SoilGrids1 km – global soil information based on automated mapping. *PLoS ONE* **9** (8), e105992.

Ho, C., Nguyen, A., Ercan, A., Kavvas, M. L., Nguyen, V. & Nguyen, T. 2018 Assessment of atmospheric conditions over the Hong Thai Binh river watershed by means of dynamically-downscaled ERA-20C reanalysis data. *Journal of Water and Climate Change* **11** (2), 540–555.

Ho, C., Trinh, T., Nguyen, A., Nguyen, Q., Ercan, A. & Kavvas, M. L. 2019 Reconstruction and evaluation of changes in hydrologic conditions over a transboundary region by a regional climate model coupled with a physically-based hydrology model: application to Thao River watershed. *Science of the Total Environment* **668**, 768–779.

Ishida, K., Kavvas, M. L., Jang, S., Chen, Z. Q., Ohara, N. & Anderson, M. L. 2014 Physically based estimation of maximum precipitation over three watersheds in northern California: atmospheric boundary condition shifting. *Journal of Hydrologic Engineering* **20** (4), 04014052.

Jang, S., Kavvas, M., Ishida, K., Trinh, T., Ohara, N., Kure, S., Chen, Z., Anderson, M., Matanga, G. & Carr, K. 2017 A performance evaluation of dynamical downscaling of precipitation over northern California. *Sustainability* **9** (8), 1457.

Kavvas, M. L., Chen, Z. Q., Dogrul, C., Yoon, J. Y., Ohara, N., Liang, L., Aksoy, H., Anderson, M. L., Yoshitani, J., Fukami, K. & Matsuura, T. 2004 Watershed environmental hydrology (WEHY) model based on upscaled conservation equations: hydrologic module. *Journal of Hydrologic Engineering* **9** (6), 450–464.

Kavvas, M. L., Yoon, J., Chen, Z. Q., Liang, L., Dogrul, E. C., Ohara, N., Aksoy, H., Anderson, M. L., Reuter, J. & Hackley, S. 2006 Watershed environmental hydrology model: environmental module and its application to a California watershed. *Journal of Hydrologic Engineering* **11** (3), 261–272.

Kavvas, M. L., Kure, S., Chen, Z. Q., Ohara, N. & Jang, S. 2013 WEHY-HCM for modeling interactive atmospheric-hydrologic processes at watershed scale. I: model description. *Journal of Hydrologic Engineering* **18** (10), 1262–1271.

Kavvas, M. L., Ishida, K., Trinh, T., Ercan, A., Darama, Y. & Carr, K. J. 2017 Current issues in and an emerging method for flood frequency analysis under changing climate. *Hydrological Research Letters* **11** (1), 1–5.

Kure, S., Jang, S., Ohara, N., Kavvas, M. L. & Chen, Z. Q. 2013 WEHY-HCM for modeling interactive atmospheric-hydrologic processes at watershed scale. II: model application to ungauged and sparsely gauged watersheds. *Journal of Hydrologic Engineering* **18** (10), 1272–1281.

Le, K. T. 2009 Tư liệu trình bày chi tiết về điều kiện tự nhiên, đặc điểm khí tượng thủy văn dòng chảy, đặc điểm khí hậu, hiện trạng kinh tế xã hội trong lưu vực sông. http://www.vncold.vn/Web/Content.aspx?distid=1862.

Loveland, T. R., Reed, B. C., Brown, J. F., Ohlen, D. O., Zhu, Z., Yang, L. W. M. J. & Merchant, J. W. 2000 Development of a global land cover characteristics database and IGBP DISCover from 1 km AVHRR data. *International Journal of Remote Sensing* **21** (6–7), 1303–1330.

Melesse, A., Weng, Q., Thenkabail, P. & Senay, G. 2007 Remote sensing sensors and applications in environmental resources mapping and modelling. *Sensors* **7** (12), 3209–3241.

Nguyen-Thi, H. A., Matsumoto, J., Ngo-Duc, T. & Endo, N. 2012 A climatological study of tropical cyclone rainfall in Vietnam. *SOLA* **8**, 41–44.

Peruccacci, S., Brunetti, M. T., Gariano, S. L., Melillo, M., Rossi, M. & Guzzetti, F. 2017 Rainfall thresholds for possible landslide occurrence in Italy. *Geomorphology* **290**, 39–57.

Poli, P., Hersbach, H., Tan, D., Dee, D., Thepaut, J. N., Simmons, A., Peubey, C., Laloyaux, P., Komori, T., Berrisford, P. & Dragani, R. 2013 *The Data Assimilation System and Initial Performance Evaluation of the ECMWF Pilot Reanalysis of the 20th-Century Assimilating Surface Observations Only (ERA-20C)*. European Centre for Medium Range Weather Forecasts.

Poli, P., Hersbach, H., Dee, D., Berrisford, P., Simmons, A. & Laloyaux, P. 2015. *ERA-20C Deterministic*. European Centre for Medium Range Weather Forecasts.

Poli, P., Hersbach, H., Dee, D. P., Berrisford, P., Simmons, A. J., Vitart, F., Laloyaux, P., Tan, D. G., Peubey, C., Thépaut, J. N. & Trémolet, Y. 2016 ERA-20C: an atmospheric reanalysis of the twentieth century. *Journal of Climate* **29** (11), 4083–4097.

Skamarock, W. C., Klemp, J. B., Dudhia, J., Gill, D. O., Barker, D. M., Wang, W. & Powers, J. G. 2005 *A Description of the Advanced Research WRF Version 2 (No. NCAR/TN-468+STR)*. National Center for Atmospheric Research Boulder Co Mesoscale and Microscale Meteorology Div.

Tachikawa, T., Kaku, M., Iwasaki, A., Gesch, D., Oimoen, M., Zhang, Z., Danielson, J., Krieger, T., Curtis, B., Haase, J. & Abrams, M. 2011 ASTER Global Digital Elevation Model Version 2–Summary of Validation Results August 31, 2011.

Tan, M., Ibrahim, A., Duan, Z., Cracknell, A. & Chaplot, V. 2015 Evaluation of six high-resolution satellite and ground-based precipitation products over Malaysia. *Remote Sensing* **7** (2), 1504–1528.

Tao, W. K., Simpson, J. & McCumber, M. 1989 An ice-water saturation adjustment. *Monthly Weather Review* **117** (1), 231–235.

Toride, K., Cawthorne, D. L., Ishida, K., Kavvas, M. L. & Anderson, M. L. 2018 Long-term trend analysis on total and extreme precipitation over Shasta Dam watershed. *Science of the Total Environment* **626**, 244–254.

Trinh, T., Ishida, K., Fischer, I., Jang, S., Darama, Y., Nosacka, J., Brown, K. & Kavvas, M. L. 2016 New methodology to develop future flood frequency under changing climate by means of physically based numerical atmospheric-hydrologic modeling. *Journal of Hydrologic Engineering* **21** (4), 04016001.

Trinh, T., Kavvas, M. L., Ishida, K., Ercan, A., Chen, Z. Q., Anderson, M. L., Ho, C. & Nguyen, T. 2018 Integrating global land-cover and soil datasets to update saturated hydraulic conductivity parameterization in hydrologic modeling. *Science of the Total Environment* **631**, 279–288.

Ward, E., Buytaert, W., Peaver, L. & Wheater, H. 2011 Evaluation of precipitation products over complex mountainous terrain: a water resources perspective. *Advances in Water Resources* **34** (10), 1222–1231.

Wuthiwongyothin, S., Jang, S. H., Ishida, K. & Kavvas, M. L. 2017 The effects of climate change on hydrology based on dynamically downscaling and physically-based hydrology model at upper Ping River Basin, Thailand. *Internet Journal of Society for Social Management Systems*. **11** (1), 78–89.

Yatagai, A., Kamiguchi, K., Arakawa, O., Hamada, A., Yasutomi, N. & Kitoh, A. 2012 APHRODITE: constructing a long-term daily gridded precipitation dataset for Asia based on a dense network of rain gauges. *Bulletin of the American Meteorological Society* **93** (9), 1401–1415.

Yokoi, S. & Matsumoto, J. 2008 Collaborative effects of cold surge and tropical depression-type disturbance on heavy rainfall in central Vietnam. *Monthly Weather Review* **136** (9), 3275–3287.

First received 22 February 2020; accepted in revised form 21 June 2020. Available online 22 July 2020